Sb-induced surface stacking faults at Ag(111) and Cu(111) surfaces: density-functional theory results

2000 J. Phys.: Condens. Matter 12 7699

(http://iopscience.iop.org/0953-8984/12/35/304)

J. Phys.: Condens. Matter **12** (2000) 7699–7704. Printed in the UK PII: S0953-8984(00)13969-4

Sb-induced surface stacking faults at Ag(111) and Cu(111) surfaces: density-functional theory results

D P Woodruff and J Robinson
Physics Department, University of Warwick, Coventry CV4 7AL, UK

Received 17 May 2000

Abstract. Using the CASTEP computer code we have conducted structural optimization calculation in the generalized-gradient approximation for the Ag(111)($\sqrt{3} \times \sqrt{3}$)R30°-Sb and Cu(111)($\sqrt{3} \times \sqrt{3}$)R30°-Sb surface phases with a view to exploring the findings of several recent experimental studies which indicate that the outermost surface alloy layer in these surfaces contains substrate and Sb atoms in the hcp hollow sites, leading to a stacking fault at the alloy–substrate interface. The results confirm that these structures do have lower total energy than the unfaulted geometries. In Ag(111) the stacking fault energy for a clean surface layer is especially low, and becomes negative in the presence of the partial Sb substitution. The relative energies of alternative Sb surface structures on Ag(111) are consistent with those of previous theoretical calculations, while the detailed geometry of the two optimal structures agrees well with experimental results.

1. Introduction

The properties of adsorbed Sb on surfaces have attracted considerable attention due to the surprising influence that this species can have on epitaxial growth, acting as a 'surfactant' in allowing layer-by-layer growth of materials which would otherwise grow as three-dimensional islands; the Sb adsorbate appears to 'float' on the surface as the material grows. One example of this phenomenon is the homoepitaxial growth of Ag on Ag(111) [1, 2], and the Ag(111)/Sb adsorption system and the Sb-aided growth have been studied extensively by a variety of experimental methods [2–5]. Of particular interest is the Ag(111)($\sqrt{3} \times \sqrt{3}$)R30°–Sb ordered surface phase formed by a nominal 0.33ML of Sb, and early investigations led to the conclusion that this probably involves substitutional adsorption of the Sb into surface Ag sites, leading to a single layer of an Ag_2Sb surface alloy. This was confirmed by total energy calculations [6, 7] which found that this substitutional site had a lower energy than any simple overlayer adsorption sites, a result which was rationalised, at least in part, by the discovery that surface vacancy formation on this surface also involves a rather low energetic penalty.

Subsequently, there have been a number of more complete quantitative experimental structure determinations of the Ag(111)($\sqrt{3} \times \sqrt{3}$)R30°–Sb structure by surface x-ray diffraction (SXRD) [8], quantitative low energy electron diffraction (LEED) [9] and medium energy ion scattering (MEIS) [10] which have all concluded that while this surface does indeed comprise a single-layer Ag_2Sb alloy, the atoms in this surface alloy layer occupy not the fcc hollow sites above Ag atoms in the third layer of the unreconstructed substrate, but are displaced laterally to occupy the hcp hollows above the second-layer Ag atoms. In effect, therefore, there is a stacking fault at the alloy–substrate interface. Moreover, similar SXRD [8] and MEIS [11] investigations of the Cu(111)($\sqrt{3} \times \sqrt{3}$)R30°–Sb surface phase have led to the conclusion

0953-8984/00/357699+06$30.00

that this structure also involves a faulted surface alloy overlayer; a further independent SXRD study of this system [12] concluded that a simple unfaulted alloy structure could be reconciled with the data, but did not consider the possibility of a faulted alloy.

In order to try to gain a better understanding of these surprising experimental results we have undertaken total energy calculations of these two surface phases. We find that the faulted alloy surface structure is indeed energetically preferred, but also show that the surface stacking fault energies are extremely low even for the two clean surfaces (and especially for Ag(111)), clearly allowing relatively subtle Sb substrate interactions to produce this surface reconstruction.

2. Computational details

The calculations presented here used the CASTEP computer code [13], which is based on density functional theory using a plane-wave pseudopotential formalism, aided by the CERIUS graphical front-end [14]. Computations were performed including gradient corrections via the generalized gradient approximation (GGA) within the local density approximation (LDA) using ultra-soft pseudopotentials. The surface net parameters used in the surface slabs were those found to give the minimum energy for bulk fcc Ag and Cu (and were within less than 1% of the experimental values). Most of the calculations of the (111)($\sqrt{3} \times \sqrt{3}$) structures used a slab of 5 layers of Ag or Cu separated by 10 Å of vacuum to produce the required three-dimensional supercell. Simple Sb overlayer structures thus contained 15 Ag or Cu atoms and one Sb atom per unit cell. Using significantly thicker slabs led to an unrealistic increase in computational time using Silicon Graphics Octane and Pentium III personal computers functioning under the LINUX operating system. However, comparative tests using 7-layer slabs were performed for many of the structures. These showed only marginal changes in the relative energies of the different structural phases, although there were some differences in the exact surface relaxation parameters, and the structural parameters presented for the optimal structures are all based on 7-layer slabs. All of the Ag/Sb results presented here are based on the 7-layer slabs but in view of the small energy changes seen in increasing the slab thickness the Cu/Sb energies are derived from 5-layer slab calculations.

For both the Ag(111) and Cu(111) surfaces the calculations conducted included the clean surface, the clean surface with a stacking fault, the clean surface with a ($\sqrt{3} \times \sqrt{3}$)R30° array of surface vacancies, and four different possible ($\sqrt{3} \times \sqrt{3}$)R30°–Sb structures. These were Sb overlayers on unreconstructed surfaces with the Sb atoms in either fcc or hcp hollow sites, and Sb substitutional alloy surface phases, also with the Sb atoms (and the Ag or Cu atoms in the alloy layer) in either fcc or hcp hollow sites (i.e. either unfaulted or faulted). In all cases the surface modifications were applied to only one face of the slab, and while the lateral dimensions of the unit mesh were constrained to the optimized bulk values, all atom positions perpendicular to the surface were allowed to relax independently within the symmetry constraints of the structures. In order to determine the absolute adsorption energies of the Sb atoms in the different structures the Sb free atom energy was also calculated using a large (10 Å) separation bulk structure and including the influence of spin-polarisation.

The influence of different k-point sampling and plane-wave energy cut-offs was explored in a series of test calculations, and this led to the bulk of the calculations for the ($\sqrt{3} \times \sqrt{3}$)R30° structures being performed with 16 symmetrically inequivalent k-points generated from an $8 \times 8 \times 2$ grid using the Monkhorst–Pack scheme, increased to 22 points from a $10 \times 10 \times 2$ grid for the (1×1) clean surface slabs. These sampling densities are similar to or finer than those used in similar published calculations such as those conducted on the Ag(111)/Sb adsorption system itself by Oppo *et al* [6]. Nevertheless, the effect of finer k-point sampling

(for example, using 31 inequivalent k-points for the clean surface models) was tested. The plane-wave kinetic energy cut-off was set to 340 eV for Ag and to 320 eV for most of the Cu calculations, although a higher value of 380 eV was also tested for Cu. In general, varying these two sets of parameter over reasonable limits led to only small changes in the differences between the total energies of the different surface structures tested.

3. Results

The first result of interest in this study is the comparative binding energies of Sb in the different surface structures. For the simple overlayer structures this (negative) binding energy is simply given as

$$\Delta E_{Sb} = E_{(111)(\sqrt{3}\times\sqrt{3})-Sb} - E_{Sb} - 3E_{(111)(1\times1)} \tag{1}$$

where E_{Sb} is the energy of the isolated Sb atom, $E_{(111)(1\times1)}$ is the energy of the clean surface (1×1) slab (which contains one Ag or Cu atom per layer) and $E_{(111)(\sqrt{3}\times\sqrt{3})}$–Sb is the energy of the $(\sqrt{3}\times\sqrt{3})$R30°–Sb slab (which contains three Ag or Cu atoms per layer plus one Sb atom). For the substitutional alloy surface phases, on the other hand, the appropriate calculation is

$$\Delta E_{Sb} = E_{(111)(\sqrt{3}\times\sqrt{3})-Sb} - E_{Sb} - 3E_{(111)(1\times1)} + E_{Ag/Cu-fcc} \tag{2}$$

because the $(\sqrt{3}\times\sqrt{3})$R30°-Sb now contains only one less Ag or Cu atoms per unit cell (two in the surface layer and three in each of the lower layers) than three times the (1×1) clean surface slab, so it is necessary to add the energy ($E_{Ag/Cu-fcc}$) of one metal atom in its bulk structure.

Table 1. Comparison of the Sb binding energies, in eV, for the four possible optimized $(\sqrt{3}\times\sqrt{3})$R30°–Sb surface structural models on Ag(111) and Cu(111).

	Ag(111)	Cu(111)
fcc overlayer	2.501	3.165
hcp overlayer	2.477	3.133
unfaulted alloy	3.379	3.840
faulted alloy	3.392	3.851

The Sb surface binding energies derived in this way are shown in table 1. Clearly the substitutional sites are significantly more favourable than the simple overlayer sites, confirming the key finding of the earlier DFT calculation for Ag(111)/Sb [6, 7]. The differences between the fcc and hcp geometries are much smaller, although for the overlayer the fcc site is favoured whereas for the alloy phase it is the hcp (faulted structure) which is favoured. Notice, however, that the energy difference between the faulted and unfaulted alloy structures is very small, being only about 12 meV per $(\sqrt{3}x\sqrt{3})R30°$ unit mesh for both metals. For comparison, the energy associated with an outermost layer stacking fault was also calculated for the two clean surfaces. The values found were 3 meV for Ag and 41 meV for Cu, in both cases per (1×1) unit mesh for 5-layer slabs; the equivalent values for the $(\sqrt{3}\times\sqrt{3})$R30° mesh are thus 9 meV and 123 meV respectively. Clearly the calculations do show the faulted structure to be energetically favoured, consistent with the experimental results, but the small energetic differences must be close to the meaningful limits of the calculations. In this regard we note that for Ag, in particular, for which the stacking fault energy for the clean surface is especially low, the exact value of this calculated energy was sensitive to the thickness of the slab. Increasing the slab thickness from 5 to 7 layer increased the stacking fault energy per (1×1) unit mesh to 9 meV but an 11-layer slab yielded a value of 5 meV.

Table 2. Comparisons of the optimized surface structural parameters (in Å) for the Ag(111)($\sqrt{3} \times \sqrt{3}$)R30°–Sb and Cu(111)($\sqrt{3} \times \sqrt{3}$)R30°–Sb faulted alloy phases found in this study with the results of experimental studies. The asterisks denote values assumed to be equal to the bulk layer spacing.

	Ag(111) this work	Ag(111) SXRD [8]	Ag(111) LEED [9]	Cu(111) this work	Cu(111) SXRD [8]	Cu(111) MEIS [11]
z_{Sb2}	2.49	2.53	2.53	2.56	2.58	2.52
z_{12}	2.47	2.50	2.46	2.09	1.98	2.05
z_{23}	2.34	2.36	2.34	2.07	2.08 *	2.08 *

While the earlier DFT calculations for the Ag(111)/Sb system did not consider the possibility of an alloy–substrate stacking fault and so are not strictly comparable, we can compare the relative and absolute Sb binding energies in the remaining phases. The relative energies are in good agreement, but this earlier study did yield significantly larger absolute values; for example, the binding energies in the fcc overlayer and fcc alloy phases were 3.26 eV and 4.49 eV to be compared with our values of 2.50 eV and 3.38 eV respectively. There are quite a number of detailed differences between the two calculations; for example the earlier calculations appeared to explore a wider range of slab thickness and adsorbed Sb onto both slab faces; they also did not allow the Ag substrate layers to relax, although this would be expected to lead to a less optimized structure and thus a smaller apparent binding energy. In general, however, these calculations are most stable in comparisons of energy differences between calculations performed in exactly the same fashion, so the fact that we agree well with the relative trends is of the greatest significance.

Comparing the results for Ag and Cu, we see that the clean surface stacking fault energy is significantly higher for Cu than for Ag. The same is true for the surface vacancy energy in a ($\sqrt{3} \times \sqrt{3}$)R30° periodicity, with the values for Ag and Sb being 495 meV and 950 meV respectively. Both of these values probably reflect the larger cohesive energy of Cu relative to Ag. These values also imply that the preference for the alloy–substrate stacking fault structure is even more surprising for the Cu(111) surface, although this is reproduced by the calculations.

Table 2 compares the surface structural parameters derived in the present calculations (for the 7-layer slabs) with those obtained in the published experimental studies. The key parameters are the outermost layer spacings, and these z values are defined in figure 1, using suffices to reflect the first (partial) and second and third (complete) substrate layers by the suffices 1, 2 and 3 and the Sb layer by the suffix Sb. The agreement is generally good. In the Ag/Sb system the effective radii expected for the Sb and Ag atoms are rather similar, so we might expect a near coplanar alloy layer. This is found both experimentally and theoretically, but the theory also reproduces the slightly larger layer spacing for Sb atoms, and the fact that this whole alloy layer is relaxed outwards relative to the underlying bulk Ag substrate (layer spacing 2.36 Å). In the case of the Cu/Sb system, on the other hand, the surface is strongly corrugated with the larger Sb atoms some 0.5 Å above the surrounding Cu atoms in the outermost layer. In this case the Cu outermost layer spacing is not significantly expanded; the calculations and the MEIS data show essentially a bulk value (2.08 Å), although the SXRD study indicates a small contraction.

4. Conclusions

Our new DFT calculations for the Ag(111)/Sb and Cu(111)/Sb ($\sqrt{3} \times \sqrt{3}$)R30° adsorption phases reproduce the surprising recent experimental results which show not only substitutional

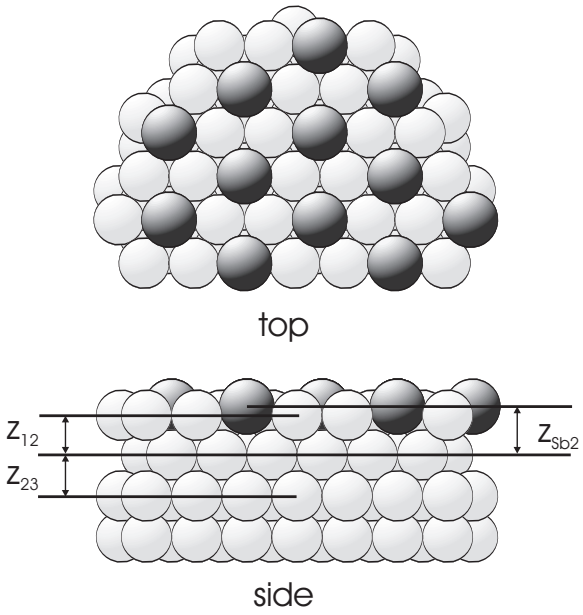

Figure 1. Schematic diagram of the faulted fcc(111)($\sqrt{3} \times \sqrt{3}$)R30°–Sb surface alloy phase including a definition of the structural parameters given in table 2.

adsorption to produce a single-layer surface alloy, but also that there is a stacking fault at the surface alloy–substrate interface. We see, however, that the energy difference between the faulted and unfaulted structures is very small, and that the possibility of creating this stacking fault is clearly eased by the very low stacking fault energy even at the clean surface. This observation is especially true for Ag(111), and in this case it is notable that a recent MEIS study finds evidence for subsurface, as well as surface layer, stacking faults [10]. Our calculations also successfully reproduce the experimental layer spacings associated with these structures. It would be interesting to explore theoretically the critical coverage of Sb which is needed to trigger this stacking fault in the surface Ag layer, but this would require the use of substantially larger surface net model structures and thus supercells with substantially larger numbers of atoms. The fact that we find the stacking fault energy to be sensitive to the slab thickness for thin slabs suggests that these calculations are only realistic using much larger scale parallel computing systems.

Acknowledgments

DPW is pleased to acknowledge the award of a Senior Fellowship by the Engineering and Physical Sciences Research Council, and also thanks David Bird, in particular, for some valuable discussions concerning the CASTEP computer code.

References

[1] van der Vegt H A, van Pinxteren H M, Lohmeier M, Vlieg E and Thornton J M C 1992 *Phys. Rev. Lett.* **68** 3335
[2] Vrijmoeth J, van der Vegt H A, .Meyer J A, Vlieg E and Behm R J 1994 *Phys. Rev. Lett.* **72** 3843

[3] Meyer J A, van der Vegt H A, Vrijmoeth J, Vlieg E and Behm R J 1996 *Surf. Sci.* **355** L375
[4] Noakes T C Q, Hutt D A, McConville C F and Woodruff D P 1997 *Surf. Sci.* **372** 117
[5] van der Vegt H A, Vrijmoeth J, Behm R J and Vlieg E 1998 *Phys. Rev. B* **57** 4127
[6] Oppo S, Fiorentini V and Scheffler M 1993 *Phys. Rev. Lett.* **71** 2437
[7] Fiorentini V, Oppo S and Scheffler M 1995 *Appl. Phys. A* **60** 399
[8] DeVries S A, Huisman W J, Goedtkindt P, Zwanenburg M J, Bennett S L, Robinson I K and Vlieg E 1998 *Surf. Sci*. **414** 159
[9] Soares E A, Bitencourt C, Nascimento V B, de Carvalho V E, de Castilho C M C, McConville C F, de Carvalho A V and Woodruff D P 2000 *Phys. Rev.* B **61** 13983
[10] Quinn P D, Brown D, Woodruff D P, Bailey P and Noakes T C Q to be published
[11] Bailey P, Noakes T C Q and Woodruff D P 1999 *Surf. Sci.* **426** 358
[12] Meunier I, Gay J-M, Lapena L, Aufray B, Oughaddou H, Landemark E, Falkenberg G, Lottermoser L and Johnson R L 1999 *Surf. Sci.* **422** 42
[13] CASTEP 3.9 academic vrsion licensed under UKCP-MSI Agreement 1999; Payne M C, Teter M P, Allen D C, Arias T A and Joannopoulos J D 1992 *Rev. Mod. Phys.***64** 1045
[14] Molecular Simulations Inc. (http://www.msi.com)